

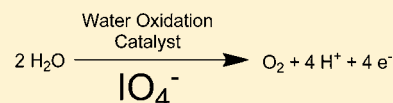
# Sodium Periodate as a Primary Oxidant for Water-Oxidation Catalysts

Alexander R. Parent, Timothy P. Brewster, Wendy De Wolf, Robert H. Crabtree,\* and Gary W. Brudvig\*

Department of Chemistry, Yale University, P.O. Box 208107, New Haven, Connecticut 06520-8107, United States

## Supporting Information

**ABSTRACT:** Sodium periodate was characterized as a primary chemical oxidant for the catalytic evolution of oxygen at neutral pH using a variety of water-oxidation catalysts. The visible spectra of solutions formed from  $\text{Cp}^*\text{Ir}(\text{bpy})\text{SO}_4$  during oxygen-evolution catalysis were measured. NMR spectroscopy suggests that the catalyst remains molecular after several turnovers with sodium periodate. Two of our  $[\text{Cp}^*\text{Ir}(\text{bis-NHC})][\text{PF}_6]_2$  complexes, along with other literature catalysts, such as the manganese terpyridyl dimer, Hill's cobalt polyoxometallate, and Meyer's blue dimer, were also tested for activity. Sodium periodate was found to function only for water-oxidation catalysts with low overpotentials. This specificity is attributed to the relatively low oxidizing capability of sodium periodate solutions relative to solutions of other common primary oxidants. Studying oxygen-evolution catalysis by using sodium periodate as a primary oxidant may, therefore, provide preliminary evidence that a given catalyst has a low overpotential.



## INTRODUCTION

Efficient conversion of solar energy into a sustainable fuel source is one of the defining challenges of the 21st century. Inorganic chemistry is playing a key role in the conversion of solar energy into fuels through the development of proton-reduction and water-oxidation catalysts. A number of water-oxidation catalysts have been developed over the past 2 decades, based on a diverse array of metals, including ruthenium,<sup>1–3</sup> manganese,<sup>4</sup> cobalt,<sup>5,6</sup> iron,<sup>7,8</sup> and iridium.<sup>9–11</sup> Complete characterization of these catalysts has proven extremely difficult, however, requiring many years, numerous techniques, and extensive computational studies to even begin to identify the mechanistic details.<sup>12</sup> Iridium-based catalysts are especially problematic because of the possibility of decomposition to iridium oxide, one of the most active water-oxidation catalysts known.<sup>11</sup>

Complicating the characterization of water-oxidation catalysts are the limitations of the standard procedures used to measure the reaction rates, specifically the use of cerium(IV) as a primary oxidant to mimic the electrochemical oxidation of the precatalyst. The use of a primary chemical oxidant facilitates rate determinations of soluble catalysts versus electrochemical methods, where only a fraction of the catalyst is active at any one time. Historically, cerium(IV) has been used as a primary oxidant in water-oxidation studies for a number of reasons, including the relative ease of interpreting its single-electron chemistry and the fact that all catalysts determined to be active using cerium(IV) have also been shown to be active electrochemically.<sup>13</sup> Severe limitations apply to the use of cerium(IV) as a primary oxidant, however. Solutions of cerium(IV) are stable only below pH  $\sim$ 3, above which the cerium(IV) spontaneously produces insoluble cerium oxides.<sup>14</sup> In addition, the standard potential of cerium(IV) is 1.70 V vs NHE, approximately 500 mV above the potential required for water oxidation at pH 0.<sup>13</sup>

The highly oxidizing conditions of cerium(IV) solutions can give rise to a number of undesirable side reactions unrelated to the electrochemical behavior of the catalyst. More disturbingly, our computational results<sup>9</sup> suggest that the  $\text{Ce}^{\text{IV}}\text{OH}^{3+}$  cation is noninnocent in the catalytic cycle by assisting proton transfer. Water oxidation with chemical oxidants does not always mimic the electrocatalytic behavior that is the most relevant for the production of solar fuels. Indeed, a variety of water-oxidation catalysts that function electrochemically are negatively affected by cerium(IV).

Sodium periodate has previously been used as the chemical oxidant for water oxidation with Fe-TAML systems,<sup>7</sup> and more recently a number of iron systems were found to show increased turnover numbers with sodium periodate relative to cerium(IV).<sup>8</sup> Additionally, sodium periodate has been shown to serve as an alternative primary oxidant to cerium(IV) in our iridium-based system, where we saw water-oxidation catalysis by a  $\text{Cp}^*\text{Ir}(\text{NHC-phenyl})$  complex.<sup>15</sup> We also found that sodium periodate drives water oxidation with Wilkinson's iridium acetate trimer under mild conditions.<sup>10</sup> In this paper, we report in detail on the properties of sodium periodate as a primary oxidant for a series of water-oxidation catalysts (the structures of some of the complexes studied are shown in Figure 1), together with its advantages and limitations.

## EXPERIMENTAL DETAILS

$[\text{Cp}^*\text{Ir}(\text{MeCN})_3][\text{PF}_6]_2$ ,<sup>16</sup> 1,1'-dimethyl-3,3'-methylene-1,2,4-ditriazolium diiodide,<sup>17</sup> and water-oxidation catalysts were made according to literature methods.<sup>1,2,4,5,9,18</sup> Deuterated solvents were purchased from Cambridge Isotope Laboratories and used as received. NMR spectra were recorded on a 500 MHz Bruker spectrometer and referenced to the residual solvent peak ( $\delta$  in ppm;  $J$  in Hz). UV–visible spectra were

Received: January 20, 2012

Published: May 15, 2012

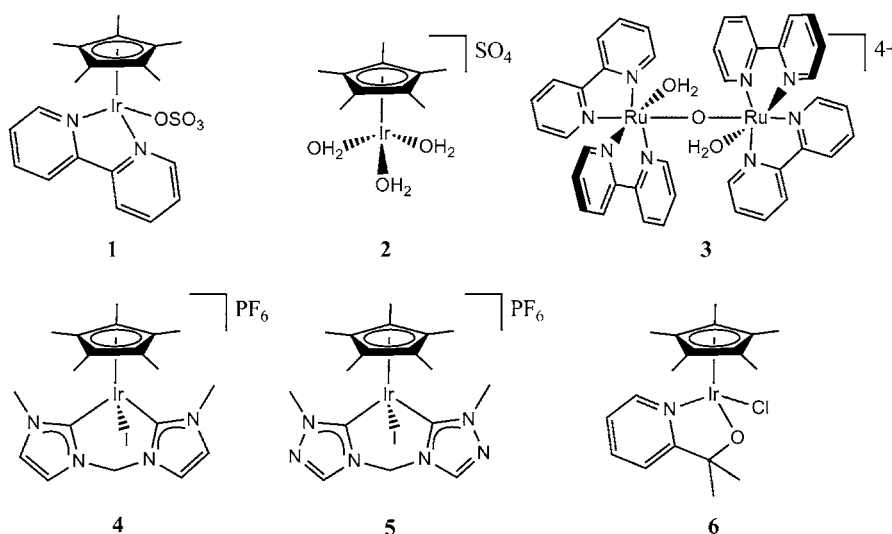


**Figure 1.** Structures of chemical complexes 1–6 studied in this paper.

recorded on a Varian Cary 50 spectrophotometer. Elemental analysis was performed by Robertson Microlit Laboratories (Ledgewood, NJ).

**General Procedure for Clark-Type O<sub>2</sub> Electrode Measurements.** A solution of sodium periodate (5.00 mL, 10.0 ± 0.2 mM) is placed in the electrode chamber, which is then sealed such that no headspace remained. Solutions were not deaerated prior to use. After the baseline has stabilized, 10.0 μL of a catalyst solution is injected into the electrode chamber with stirring, and the change in the electrode current over time is recorded. This procedure is repeated a minimum of three times per reaction condition. Error bars shown in figures in the Supporting Information represent 2 standard deviations from the mean and are generally between 10 and 20% of the measured value.

**Procedure for Gas Chromatography–Mass Spectrometry (GC–MS) Analysis.** A solution of 1.6 mM catalyst and a solution of oxidant [10 mM for NaIO<sub>4</sub> and 70 mM for cerium(IV) ammonium nitrate (CAN)] were placed under vacuum. The solutions were rapidly mixed with stirring and allowed to stand for approximately 5 min. The reaction headspace was then transferred into a cold trap prior to sampling with a Stanford Research Systems Residual Gas Analyzer gas chromatograph–mass spectrometer.

**Procedure for Dynamic Light-Scattering Analysis.** A catalyst solution was added to a 10 mM solution of sodium periodate and allowed to react for 20 min. Final catalyst concentrations were ~330 μM. The samples were then analyzed on a Malvin Zetasizer Nano instrument.

**Synthesis of [Cp\*Ir(bistriazolium)]PF<sub>6</sub> (5).** A 100 mL Schlenk flask was charged with 614 mg (0.829 mmol) of [Cp\*Ir(MeCN)<sub>3</sub>][PF<sub>6</sub>]<sub>2</sub> and 359 mg (0.829 mmol) of 1,1'-dimethyl-3,3'-methylene-1,2,4-ditriazolium diiodide. The flask was placed under nitrogen, and 24 mL of dry acetonitrile was added via a syringe. A total of 0.35 mL (2.50 mmol, 3 equiv) of triethylamine was then added. The reaction was stirred at 60 °C for 48 h. After completion, the solution was cooled to room temperature and the solvent removed. The resulting orange powder was redissolved in dry chloroform and cooled to –78 °C for 1 h. A pale-yellow precipitate formed and was collected by vacuum filtration, washed with cold diethyl ether, and dried in vacuo overnight. Yield: 572 mg (0.735 mmol, 89%). <sup>1</sup>H NMR (500 MHz, CD<sub>3</sub>CN): δ 8.43 (s, 2H), 6.33 (d, *J* = 13.3 Hz, 1H), 5.53 (d, *J* = 13.3 Hz, 1H), 3.92 (s, 6H), 1.96 (s, 15H). <sup>13</sup>C NMR (126 MHz, CD<sub>3</sub>CN): δ 151.06, 142.38, 94.60, 57.94, 40.84, 8.70. Elem. anal. Calcd.: C, 26.19; H, 3.49; N, 10.78. Found: C, 26.31; H, 2.73; N, 10.51.

## RESULTS

**Characterization of the Catalytic Activity of 1 with Sodium Periodate.** Following our finding that sodium periodate can drive catalytic water oxidation with both

Wilkinson's iridium acetate trimer and our Cp\*Ir(NHC) complex,<sup>10,15</sup> we began to explore its application to other systems such as our own recently reported [Cp\*Ir(bpy)SO<sub>4</sub>] (1; Figure 1).<sup>9</sup> Upon the addition of 1 to a solution of sodium periodate, oxygen begins to evolve with an increasing rate, reaching a maximum after ~5 min (Figure 2). This maximum

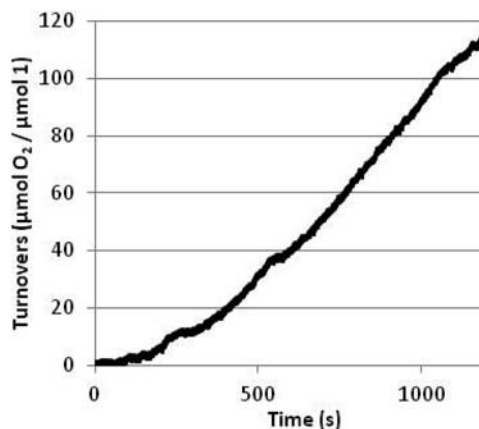


**Figure 2.** Turnovers of oxygen versus time for a 473 nM solution of 1 in 20.4 mM sodium periodate as measured using a Clark electrode at pH ca. 5.3.

rate is maintained for at least 1 h and was used to analyze the kinetic behavior of the system. Over the course of the reaction, the pH of the solution was found to decrease from 5.35 to 5.25. As shown in Figures S1 and S2 in the Supporting Information, the oxygen-evolution turnover frequency of compound 1 exhibits first-order dependence with respect to the catalyst concentration, as was also seen previously when cerium(IV) was used as a primary oxidant.<sup>9</sup>

In order to determine whether the observed oxygen produced was the result of water oxidation or sodium periodate dismutation, i.e., reaction of periodate rather than water with an Ir<sup>V</sup>=O species, kinetic studies were performed. A first-order relationship between the rate of oxygen evolution and the concentration of periodate in solution is observed (Figures S3 and S4 in the Supporting Information). This result is consistent with several pathways. One is oxidation of the catalyst in the

rate-determining step of the catalytic cycle where first-order dependence on the oxidant concentration would be expected at low oxidant concentrations. Another is the rate-determining reaction of free periodate with a  $[\text{Cp}^*\text{Ir}(\text{bpy})\text{IO}_4]$  intermediate, where first-order dependence on the periodate concentration would be expected at high concentrations. Ideally, one could resolve this ambiguity by extending the range of concentrations of periodate measured because the two mechanisms predict different behavior at high and low concentrations, respectively. In the case of water-oxidation catalysis by the manganese terpyridyl dimer driven by oxone, a saturation behavior at high oxone concentration is observed, supporting a mechanism in which the rate-determining step is oxidation of the catalyst to form a reactive high-valent intermediate that rapidly evolves oxygen.<sup>19</sup> Unfortunately, in the case of the oxygen-evolution reaction of **1** driven by periodate, it was not possible to extend the range of concentrations sufficiently to differentiate the two mechanisms. At the low end of concentrations, the rate of oxygen evolution becomes too small to measure accurately, and the limited solubility of sodium periodate at neutral pH prevents measurements at the high end. Oxygen isotope labeling could also be used to remove this ambiguity; unfortunately, sodium periodate undergoes rapid oxo exchange with water,<sup>20</sup> preventing meaningful analysis of the oxygen isotope data. In this case, we must, therefore, work by analogy from the previous data using cerium(IV) and electrochemistry, demonstrating that **1** is indeed capable of catalytic water oxidation.<sup>9</sup>

**Comparison of the Activity of **1** with Periodate versus CAN.** It has recently been suggested that  $\text{Cp}^*\text{Ir}$  complexes such as **1** undergo rapid degradation in the presence of cerium(IV).<sup>21</sup> We, thus, made efforts to determine whether nanoparticles were formed while using sodium periodate. In contrast to cerium(IV) as a primary oxidant for **1**, where a decrease in the oxygen productivity over time is observed,<sup>9</sup> periodate permits oxygen production over extended periods (Figure 2). This suggests that **1** has improved stability in sodium periodate solutions, which may be due to either the lower redox potential of periodate relative to cerium(IV) or the higher pH at which the experiments are run. Further evidence on this point was obtained from tandem oxygen and carbon dioxide detection during turnover using GC–MS. Upon the addition of a solution of **1** to a solution of CAN at pH ca. 0.9, both oxygen and carbon dioxide are detected in the headspace by GC–MS, showing ligand degradation to carbon dioxide. The addition of a solution of **1** to a solution of sodium periodate at pH ca. 5.35, however, results in substantial amounts of oxygen production but no detectable carbon dioxide production, despite multiple freeze–thaw cycles to remove any dissolved  $\text{CO}_2$ . This demonstrates that any decomposition of **1** with periodate must be substantially less extensive than that with cerium(IV), which may be either due to a lower rate of decomposition using periodate or due to the lower concentrations of oxidant required in experiments using periodate.

**Confirming the Homogeneity of **1** with Periodate.** It has recently been suggested that at high concentrations **1** decomposes into a heterogeneous material upon treatment with cerium(IV), which is then responsible for the observed water-oxidation catalysis.<sup>21</sup> In order to better characterize the catalytic cycle of the complex and to check for the formation of heterogeneous material using sodium periodate, UV–visible spectral time-course studies were conducted. Figure 3 shows that a peak at 580 nm forms over the course of the first 3 min

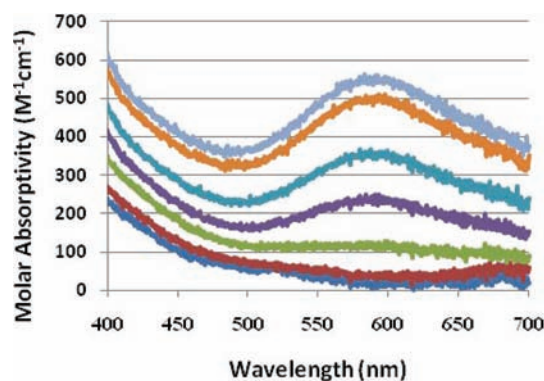


**Figure 3.** Visible spectrum of a solution of  $105 \mu\text{M}$  **1** over time after the addition of  $8.7 \text{ mM}$  sodium periodate. Time points: 19 s, 1.3 min, 3.3 min, 6.8 min, 9.3 min, 12.3 min, and 13.3 min.

of the reaction and reaches a maximum after  $\sim 12$  min, in addition to a rising baseline due to vigorous bubble formation. This corresponds to the slow induction observed in the Clark-electrode experiment (Figure 2) and is consistent with the 580 nm band belonging to a steady-state iridium(IV) form of the catalyst, indicating slow oxidation of the iridium(III) species to a high-valent iridium species, followed by rate-determining O–O bond formation. The addition of ethanol causes the 580 nm band to disappear over the course of  $\sim 5$  min with the formation of a species that exhibits absorption at  $\sim 430$  nm (Figure 4). This observation indicates that ethanol reduces the

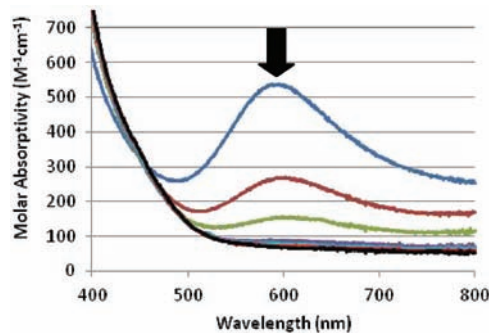


**Figure 4.** Visible spectrum of a solution of  $105 \mu\text{M}$  **1** and  $8.7 \text{ mM}$  sodium periodate (initial concentrations) over time after the addition of ethanol. Time points: 0 s, 45 s, 2.25 min, 4.75 min, 6.25 min, 9.25 min, and 11.75 min.

steady-state high-valent iridium species to iridium(III). Importantly, the 580 nm band cannot be assigned to conventional iridium dioxide nanoparticles, which are not reduced by ethanol.

To confirm that no iridium oxide nanoparticles are formed upon the reaction of **1** with periodate, dynamic light-scattering experiments were conducted. No nanoparticles within the detection limit of the instrument were found to be present in a solution of **1** 20 min after the reaction with periodate. To ensure that the instrument was capable of detecting iridium dioxide nanoparticles under the reaction conditions, a solution of  $\text{IrCl}_3$  was combined with sodium periodate and allowed to stand for 20 min before measurement. The  $\text{IrCl}_3$  solution clearly shows that large numbers of nanoparticles have formed (Figure S5 in the Supporting Information), demonstrating that if **1** were forming nanoparticles similarly to  $\text{IrCl}_3$ , they should be detectable by the dynamic light-scattering instrument.

We then considered whether an alternative form of iridium oxide, such as the “blue layer” (BL) we have previously reported, could be forming.<sup>22</sup> We, therefore, oxidized a solution of Cp\*Ir(H<sub>2</sub>O)<sub>3</sub> (**2**), the precursor to BL, with sodium periodate and monitored the visible spectra of the solution over time. The expected 580 nm band corresponding to BL was observed after approximately 15 min. Upon the addition of ethanol to the solution, however, the 580 nm band persisted with only a small decrease in the intensity, indicating that the oxidation product of **2** is not readily reduced by ethanol (Figure 5). Additionally, the 580 nm band formed when **1** is oxidized

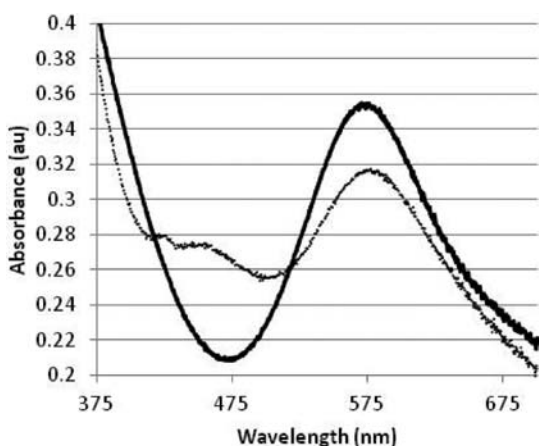


**Figure 5.** Solution of 274  $\mu\text{M}$  **2** in 8.8 mM sodium periodate for 1 h before (solid line) and after the addition of ethanol (dashed line). Absorbance values corrected for dilution.

by periodate appears slowly over the first 15 min of reaction (Figure 3). In contrast the 580 nm band formed from **2** appears abruptly, suggesting autocatalytic nanoparticle formation in the case of **2** but not of **1**. Thus, the 580 nm peak formed upon periodate oxidation of **1** is distinct from the one coming from BL-like nanoparticles, which form upon oxidation of **2** in solution (Figure S6 in the Supporting Information). On the basis of these results, combined with the data collected showing no nanoparticle formation when **1** is oxidized by periodate, we conclude that the 580 nm peak observed for **1** is from a molecular high-valent iridium species.<sup>23</sup>

#### Analysis of the Catalyst after Reaction with Periodate.

In order to gain insight into the active form of the catalyst, we attempted recovery of **1** after the reaction with sodium periodate and were able to recover a yellow powder after the reaction of **1** with 100 equiv of sodium periodate by quenching with ethanol and removal of the solvent via rotary evaporation. Instead of a single Cp\* methyl resonance in the NMR, the yellow powder exhibits three separate peaks in the aliphatic region, indicating that, while at least some of the Cp\* remains even after 50 turnovers, partial oxidative modification has occurred (Figure S7 in the Supporting Information). Additionally, the bipyridyl NMR resonances have broadened and shifted slightly downfield relative to the starting catalyst, indicating that no unmodified **1** remains after 50 turnovers. The peak broadening of the bipyridyl resonances differ in extent in CD<sub>3</sub>OD and D<sub>2</sub>O, suggesting that it results from ligand exchange at the iridium center. This is consistent with recent reports that the initial oxidation product of Cp\*Ir water-oxidation complexes is hydroxylation of the Cp\* ring, leading to a modified ring that can displace solvent bound to iridium.<sup>24</sup>

No free bipyridine is observed in the NMR spectra, however, suggesting that **1** has not decomposed to a nanoparticulate material to any significant extent. IR analysis of the yellow powder shows a broad peak at 1640 cm<sup>-1</sup> (Figures S7 and S8 in the Supporting Information), indicating the formation of a carbonyl in the oxidation product, which may be assigned to a carboxylic acid due to the absence of aldehyde protons in the NMR.

**Reaction of 6 with Periodate.** Although it has not been possible to definitively eliminate periodate rather than water being the source of the O<sub>2</sub> because of fast water–periodate O atom exchange, we have been able to obtain indications from a comparison between **1** and **6**. In contrast to the case of **1**, the reaction of **6** with periodate to form O<sub>2</sub> proceeds without an induction period. Additionally, the rate of the reaction was found to be approximately 2 orders of magnitude faster than that for **1**, despite similar reaction rates for the two complexes when cerium(IV) is used as the primary oxidant.<sup>9,25</sup> This likely results from deprotonation of the substrate water by the internal base alkoxy function of the pyridine alkoxide complex **6** at the near-neutral pH of the NaIO<sub>4</sub> study. In contrast, at the acid pH of the cerium(IV) study, the alkoxide is likely to be protonated and incapable of deprotonating substrate water. This mechanism is similar to the one believed to operate when using periodate to drive water oxidation with iridium dioxide and with Wilkinson’s iridium acetate trimer in the presence of excess acetate.<sup>10</sup> The large difference in rate between **6**, **2**, and prepared iridium dioxide nanoparticles argues against decomposition of the complex to an iridium oxide material over short time periods because the observed rate should decrease sharply if that were occurring.

**Screening Literature Water-Oxidation Systems for Activity with Periodate.** After finding that **1**, **2**, and **6** are competent water-oxidation precatalysts with periodate, we were encouraged to assay a number of other catalytic systems to determine the general applicability of periodate as a primary chemical oxidant for water oxidation. Interestingly, most of the catalysts that we tested showed no catalytic water-oxidation activity using sodium periodate at pH ca. 5.4. Specifically, the manganese terpyridyl dimer,<sup>4</sup> Hill’s cobalt polyoxometallate,<sup>5</sup> and [Ru(4'-EtO-terpy)(bpy)(OH<sub>2</sub>)](NO<sub>3</sub>)<sub>2</sub><sup>3</sup> showed no reaction upon addition to a solution of sodium periodate.

Meyer’s blue dimer<sup>2</sup> (**3**) showed no detectable oxygen-evolution activity with periodate; however, a color change from blue to orange was observed corresponding to the 646 nm peak of the III,III state of **3** converting to the 490 nm peak of the III,IV state (Figure 6).<sup>26</sup> Oxygen evolution was detected using other iridium catalysts, however, including iridium acetate,<sup>10</sup> [Cp\*Ir(bisimidazole)I][PF<sub>6</sub>]<sub>2</sub> (**4**),<sup>15</sup> compound **5**, and iridium dioxide nanoparticles.

**Reaction of 3 with Periodate.** Examination of the visible spectral changes of **3** upon addition to periodate reveals important information about the characteristics of periodate as an oxidant. First, the oxidation of **3** from Ru<sup>III,III</sup> to Ru<sup>III,IV</sup> is a one-electron process, suggesting that periodate is serving as a one-electron oxidant. The ability of periodate to act as a one-electron oxidant has been previously demonstrated with hexaaquairon(II).<sup>27</sup> In the case of **3**, it is not possible to exclude an initial two-electron oxidation, followed by a bimolecular electron-exchange reaction; however, no oxygen generation is observed, as may be expected if a ruthenium(V) species were generated. Second, the lack of observable oxygen formation by **3** when added to periodate suggests that periodate

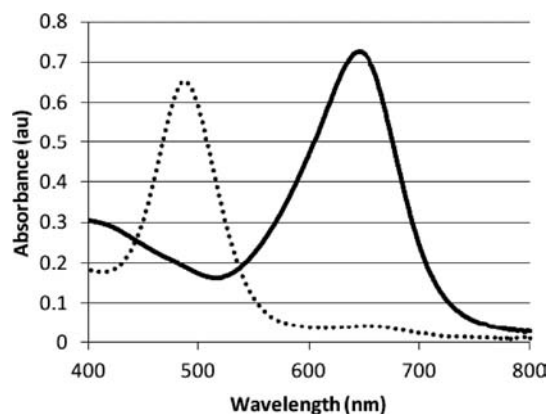


**Figure 6.** Visible spectra of 44  $\mu\text{M}$  **3** before (solid line) and after the addition of 1.2 mM sodium periodate (dotted line).

disproportionation does not contribute significantly to the oxygen produced by the iridium systems because **3** is known to catalyze the disproportionation of hypochlorite.<sup>28</sup>

## DISCUSSION

Because both the reduction of periodate to iodate and the oxidation of water to oxygen require one proton per electron, the overpotential provided by periodate is constant at approximately 420 mV from pH 2 to 8. Periodate is, thus, an approximately 20% less powerful oxidant than cerium(IV) and ozone for water oxidation, which accounts for the inability of periodate to serve as a primary oxidant for complex **3** and the manganese terpyridyl dimer (Table 1). The  $[\text{Ru}(4'\text{-EtO-}$

**Table 1.** Turnover Frequencies of Catalysts Measured with 10 mM Sodium Periodate (2 Standard Deviation Error Approximately 10% of Mean; NR = no reaction)

catalyst	TOF ( $\text{s}^{-1}$ )	catalyst concn ( $\mu\text{M}$ )
<b>1</b>	0.042	0.47
<b>2</b>	0.060	4.9
<b>3</b>	NR	
<b>4</b>	0.13	2.4
<b>5</b>	0.20	2.2
<b>6</b>	2.20	0.10
$\text{Co}_4(\text{H}_2\text{O})_2(\text{PW}_9\text{O}_{34})_2^{10}$	NR	
$[\text{Ir}_3(\text{OAc})_6(\text{H}_2\text{O})_3]^+$	0.27 <sup>*,10</sup>	0.12
iridium dioxide nanoparticles	0.38 <sup>*,10</sup>	0.43
$[\text{Mn}(\text{terpy})\text{O}(\text{H}_2\text{O})_2(\text{NO}_3)_3$	NR	
$[\text{Ru}(4'\text{-EtO-terpy})(\text{bpy})(\text{OH}_2)](\text{NO}_3)_2$	NR	
$[\text{Fe}(\text{OTf})_2(\text{mcp})]$	0.061 <sup>8</sup>	12.5

\*In the presence of 23 mM sodium acetate buffer, turnovers per iridium center.

$\text{terpy})(\text{bpy})(\text{OH}_2)](\text{NO}_3)_2$  system was not expected to generate oxygen given its  $\sim 480$  mV required overpotential. The lack of reaction of periodate with Hill's cobalt polyoxometallate (Table 1) is a more complex case because previous studies were conducted at pH 8, unlike those conducted here at pH 5.3, because periodate begins to form  $\text{H}_2\text{I}_2\text{O}_{10}$  at pH 8.<sup>29</sup> Thus, the failure of periodate to effect water oxidation with the polyoxometallate may result from the difference in pH. It should also be noted, however, that at pH 8, where the original studies on the cobalt polyoxometallate complex were done, the overpotential of the  $\text{Ru}(\text{bpy})_3^{3+}$

oxidant is 472 mV. Thus, the observed inactivity may result from the lower overpotential of periodate as seen with the other complexes. On the other hand, periodate may be able to serve as a primary oxidant in the case of the iridium and iron systems because their potentials for oxidation are below that which periodate can provide. Thus, sodium periodate may be selective for water-oxidation catalysts with relatively low overpotentials.

Despite the success in using sodium periodate to drive our  $\text{Cp}^*\text{Ir}$  systems, there are a number of drawbacks that prevent its general use as a primary oxidant. The most important concern is the possibility for periodate dismutation to contribute to the observed oxygen evolution, i.e., attack of periodate rather than water on an iridium oxo species. Checking for dismutation is complicated by the rapid oxo exchange between periodate and water mediated by the meta-para periodate equilibrium.<sup>20</sup> Alternative primary oxidants may be used to conclusively demonstrate the water-oxidation ability of the catalyst, and the rate dependence of the reaction on the periodate concentration may be measured; however, it remains difficult to prove conclusively that oxygen produced when using periodate is from water. Further complications arise when using sodium periodate to obtain mechanistic information about a complex because others have demonstrated that it can serve as both a one- and two-electron oxidant.<sup>27</sup> This complicates mechanistic interpretations and computational studies by allowing for numerous plausible oxidation mechanisms. In addition, iodate is formed as periodate is consumed and may serve as either a ligand or a weak oxidant in its own right.

Periodate remains useful as a primary oxidant, however, as long as studies are planned with its drawbacks in mind. Periodate maintains a constant overpotential in the pH range of 2–7. As demonstrated for **6**, the ability to screen catalytic activity at multiple pH values can provide mechanistic insight. In addition, because of periodate's relatively low oxidizing power, it is selective for water-oxidation catalysts having low overpotentials and appears less prone to causing catalyst decomposition than harsher oxidants such as cerium(IV).

## CONCLUSIONS

The use of sodium periodate rather than cerium(IV) as a sacrificial oxidant for studying water-oxidation catalysts has been shown to lead to reduced degradation of the catalysts. This is, in part, because of the higher pH at which measurements can be run and, in part, because of the lower oxidizing power of periodate relative to cerium(IV) solutions. Because of the lower oxidizing power of sodium periodate, it only functions to drive turnover for water-oxidation catalysts with relatively low overpotentials. Sodium periodate can, thus, be used as a preliminary screen for water-oxidation catalysts with low overpotentials. For catalysts with higher overpotentials, sodium periodate can potentially be used to access intermediate species in the catalytic cycle without driving complete turnover, allowing for more detailed analysis of those species.

## ASSOCIATED CONTENT

### Supporting Information

Kinetic plots, dynamic light-scattering data, and NMR and IR spectra. This material is available free of charge via the Internet at <http://pubs.acs.org>.

## AUTHOR INFORMATION

### Corresponding Author

\*E-mail: robert.crabtree@yale.edu (R.H.C.), gary.brudvig@yale.edu (G.W.B.).

### Notes

The authors declare no competing financial interest.

## ACKNOWLEDGMENTS

This study was supported as part of the Argonne–Northwestern Solar Energy Research (ANSER) Center, an Energy Frontier Research Center funded by the U.S. Department of Energy, Office of Science, Office of Basic Energy Sciences, under Award DE-SC0001059. A.R.P. was funded by an NSF graduate research fellowship. The authors thank Dr. Etsuko Fujita, Dr. Dmitriy Polyanski, and Dr. Jonathan Hull of Brookhaven National Laboratory for their assistance with the tandem mass spectrometry measurements and Dr. Dmytro Nykypanchuk of the Brookhaven National Laboratory Center for Functional Nanomaterials for assistance with dynamic light-scattering measurements (Rapid Access Proposal No. 31015). The authors also thank James D. Blakemore and Nathan D. Schley for fruitful discussions.

## REFERENCES

- (1) Concepcion, J. J.; Jurss, J. W.; Templeton, J. L.; Meyer, T. J. *J. Am. Chem. Soc.* **2008**, *130*, 16462–16463.
- (2) Gersten, S. W.; Samuels, G. J.; Meyer, T. J. *J. Am. Chem. Soc.* **1982**, *104*, 4029–4030.
- (3) Yagi, M.; Tajima, S.; Komi, M.; Yamazaki, H. *Dalton Trans.* **2011**, *40*, 3802.
- (4) Limburg, J.; Vrettos, J. S.; Liable-Sands, L. M.; Rheingold, A. L.; Crabtree, R. H.; Brudvig, G. W. *Science* **1999**, *283*, 1524–1527.
- (5) Yin, Q.; Tan, J. M.; Besson, C.; Geletii, Y. V.; Musaev, D. G.; Kuznetsov, A. E.; Luo, Z.; Hardcastle, K. I.; Hill, C. L. *Science* **2010**, *328*, 342–345.
- (6) Kanan, M. W.; Nocera, D. G. *Science* **2008**, *321*, 1072–1075.
- (7) Ellis, W. C.; McDaniel, N. D.; Bernhard, S.; Collins, T. J. *J. Am. Chem. Soc.* **2010**, *132*, 10990–10991.
- (8) Fillol, J. L.; Codolà, Z.; Garcia-Bosch, I.; Gómez, L.; Pla, J. J.; Costas, M. *Nat. Chem.* **2011**, *3*, 807–813.
- (9) Blakemore, J. D.; Schley, N. D.; Balcells, D.; Hull, J. F.; Olack, G. W.; Incarvito, C. D.; Eisenstein, O.; Brudvig, G. W.; Crabtree, R. H. *J. Am. Chem. Soc.* **2010**, *132*, 16017–16029.
- (10) Parent, A. R.; Blakemore, J. D.; Brudvig, G. W.; Crabtree, R. H. *Chem. Commun.* **2011**, *47*, 11745–11747.
- (11) Nakagawa, T.; Beasley, C. A.; Murray, R. W. *J. Phys. Chem. C* **2009**, *113*, 12958–12961.
- (12) Concepcion, J. J.; Jurss, J. W.; Brennaman, M. K.; Hoertz, P. G.; Patrocinio, A. O. T.; Murakami Iha, N. Y.; Templeton, J. L.; Meyer, T. *J. Acc. Chem. Res.* **2009**, *42*, 1954–1965.
- (13) Mills, A. *Chem. Soc. Rev.* **1989**, *18*, 285–316.
- (14) Hayes, S. A.; Yu, P.; O’Keefe, T. J.; O’Keefe, M. J.; Stoffer, J. O. *J. Electrochem. Soc.* **2002**, *149*, C623–C630.
- (15) Brewster, T. P.; Blakemore, J. D.; Schley, N. D.; Incarvito, C. D.; Hazari, N.; Brudvig, G. W.; Crabtree, R. H. *Organometallics* **2011**, *30*, 965–973.
- (16) White, C.; Yates, A.; Maitlis, P. M. *Inorg. Synth.* **1992**, *29*, 228–229.
- (17) Unger, Y.; Meyer, D.; Strassner, T. *Dalton Trans.* **2010**, *39*, 4295.
- (18) Vogt, M.; Pons, V.; Heinekey, D. M. *Organometallics* **2005**, *24*, 1832–1836.
- (19) Limburg, J.; Vrettos, J. S.; Chen, H.; de Paula, J. C.; Crabtree, R. H.; Brudvig, G. W. *J. Am. Chem. Soc.* **2001**, *123*, 423–430.
- (20) Pecht, I.; Luz, Z. *J. Am. Chem. Soc.* **1965**, *87*, 4068–4072.

- (21) Grotjahn, D. B.; Brown, D. B.; Martin, J. K.; Marelius, D. C.; Abadjian, M.-C.; Tran, H. N.; Kalyuzhny, G.; Vecchio, K. S.; Specht, Z. G.; Cortes-Llamas, S. A.; Miranda-Soto, V.; van Niekerk, C.; Moore, C. E.; Rheingold, A. L. *J. Am. Chem. Soc.* **2011**, *133*, 19024–19027.
- (22) Blakemore, J. D.; Schley, N. D.; Olack, G. W.; Incarvito, C. D.; Brudvig, G. W.; Crabtree, R. H. *Chem. Sci.* **2011**, *2*, 94–98.
- (23) Castillo-Blum, S. E.; Richens, D. T.; Sykes, A. G. *Inorg. Chem.* **1989**, *28*, 954–960.
- (24) Savini, A.; Belanzoni, P.; Bellachioma, G.; Zuccaccia, C.; Zuccaccia, D.; Macchioni, A. *Green Chem.* **2011**, *13*, 3360–3374.
- (25) Schley, N. D.; Blakemore, J. D.; Subbaiyan, N. K.; Incarvito, C. D.; D’Souza, F.; Crabtree, R. H.; Brudvig, G. W. *J. Am. Chem. Soc.* **2011**, *133*, 10473–10481.
- (26) Gilbert, J. A.; Eggleston, D. S.; Murphy, W. R.; Geselowitz, D. A.; Gersten, S. W.; Hodgson, D. J.; Meyer, T. J. *J. Am. Chem. Soc.* **1985**, *107*, 3855–3864.
- (27) El-Eziri, F. R.; Sulfab, Y. *Inorg. Chim. Acta* **1977**, *25*, 15–20.
- (28) Raven, S. J.; Meyer, T. J. *Inorg. Chem.* **1988**, *27*, 4478–4483.
- (29) Weavers, L. K.; Hua, I.; Hoffmann, M. R. *Water Environ. Res.* **1997**, *69*, 1112–1119.